Effect of the Aggregation Structure on the Thermal Shrinkage of Polyacrylonitrile Fibers during the Heat-Treatment Process

Bin Wang, Chun Zhao, Shijie Xiao, Jing Zhang, Lianghua Xu

National Carbon Fiber Engineering Research Center, Beijing University of Chemical Technology, Beijing 100029, People's Republic of China

Received 24 July 2011; accepted 20 September 2011
DOI 10.1002/app.35648
Published online in Wiley Online Library (wileyonlinelibrary.com).

ABSTRACT: Secondary thermal shrinkage or chemical shrinkage involved in the thermal shrinkage of polyacrylonitrile (PAN) fibers was not only associated with the cyclization degree but also the thermal mobility of molecular chains in the aggregation structures during crosslinking. In this study, the cyclization process was monitored with differential scanning calorimetry and IR spectroscopy. The evolution of aggregation structures throughout cyclization and variations in the secondary shrinkage for the PAN fibers were characterized with wide-angle X-ray diffraction and thermal mechanical analysis, respectively. The results show that with increasing temperature, the cyclization degree increased; the cyclization occurred first in amorphous regions and then extended to the crystalline regions. Correspondingly, the secondary shrinkage also increased and could be separated into two stages: those of the amorphous and crystalline phases. The shrinkage of the crystalline regions was much bigger than that of the amorphous regions. For fibers with different aggregation structures, the crystallinity affected the cyclization degree in the amorphous and crystalline regions and resulted in the difference in total shrinkage. Furthermore, because the unoriented molecular chains in both the amorphous and crystalline regions shrank more after cyclization, the shrinkage of both regions was primarily decided by the level of orientated molecular chains participating in the cyclization. © 2012 Wiley Periodicals, Inc. J Appl Polym Sci 000: 000–000, 2012

Key words: crosslinking; crystal structures; thermal properties

INTRODUCTION

The macroscale shrinkage behavior of polyacrylonitrile (PAN) fibers throughout thermal treatment reflects physical and chemical changes in the molecular chains. Warner and coworkers[1–3] found that the overall shrinkage of PAN fibers could be classified into two stages: initial shrinkage and secondary shrinkage. The initial shrinkage is a totally physical process and is also called *entropic shrinkage;* it is caused by the relaxation of molecular chains in the amorphous phase.[4–6] The secondary shrinkage (chemical shrinkage) is mainly due to the crosslinking of molecular chains via chemical reactions. However, in this process, the original crystalline structure is destroyed and the molecular chains are disoriented, so the effect of aggregation transformation on the secondary shrinkage should not be ignored.

Many researchers have studied the effects of chemical reaction mechanisms on the secondary shrinkage by changing the comonomers of PAN fibers, the atmosphere of the thermal treatment, the heating rate, and so on.[7–13] In fact, because the aggregation structure dramatically affects the thermal mobility of molecular chains, it is important to understand the evolution of aggregation structures throughout the chemical reactions. The effects of the thermal mobility of the molecular chains in different aggregation structures on the shrinkage of PAN fibers during the crosslinking process is also important for revealing the thermal shrinkage mechanism of PAN fibers.

In this study, a series of experiments were designed to probe the thermal shrinkage behaviors of PAN fibers under a nitrogen atmosphere. The corresponding changes in the aggregation structure throughout these thermal treatments were measured with wide-angle X-ray diffraction (WAXD), and the effects of aggregation structures on the secondary shrinkage of PAN fibers were analyzed.

EXPERIMENTAL

Materials

Four types of PAN precursor containing itaconic acid copolymer (≤1%) were produced by variation of the stretching ratio during wet spinning. The aggregation

Correspondence to: L. Xu (xulh@mail.buct.edu.cn).
Contract grant sponsor: National Basic Research Program of China; contract grant number: 2011CB605602.

© 2012 Wiley Periodicals, Inc.

TABLE I
Parameters for the Aggregation Structures of the PAN Fibers

Sample number	$X_{0,cry}$ (%)	$f_{0,sum}$ (%)	$f_{0,cry}$ (%)	$f_{0,amo}$ (%)
1	55.7	67.2	85.7	43.9
2	56.6	68.3	86.1	45.1
3	57.9	70.3	87.0	47.3
4	59.4	74.0	88.4	52.9

$X_{0,cry}$, crystallinity; $f_{0,sum}$, total chain orientation degree; $f_{0,cry}$, orientation degree of the crystalline region; $f_{0,amo}$, orientation degree of the amorphous region.

structure parameters for these samples are shown in Table I. The details for the calculation are described later.

Thermal mechanical analysis (TMA)

The thermal shrinkage of the PAN fibers was measured by TMA with a TA Instruments Q400 (New Castle, DE, USA). The fibers were tied vertically in a special holder within the instrument with specified initial lengths (the initial values for these fibers are listed in Table II). The thermal treatment process was performed at a heating rate of 10°C/min in N_2 from 50 to 300°C. The shrinkage rate (ΔL) of the PAN fiber was calculated with Eq. (1):

$$\Delta L = \frac{L_T - L_0}{L_0} \times 100\% \quad (1)$$

where L_T is the length of the PAN fiber at temperature T and L_0 is the initial length of the PAN fiber.

Differential scanning calorimetry (DSC) measurements

The chemical reaction enthalpy measurements of the PAN fibers during the heating process were performed on a DSC instrument (TA Instruments Q100). The PAN precursors were cut to short fibers and then sealed in aluminum pans. Each sample was about 4 mg. The thermal treatment process was carried out at a heating rate of 10°C/min under an N_2 atmosphere from 50 to 300°C. The relative cyclization degree (RCD) of the stabilized PAN fiber was calculated by Eq. (2):[14]

$$\mathrm{RCD} = \frac{\Delta H}{H_0} \times 100\% \quad (2)$$

where H_0 is the total chemical reaction enthalpy for PAN precursors and could be obtained from the integration of the exothermic peak and ΔH is the enthalpy of the reaction that already occurred at a given temperature.

WAXD measurements

WAXD measurements were performed with a PANalytical X'Pert PRO Multi Purpose X-ray Diffractometer instrument equipped with a PIXcel detector with a high dynamic range (25 million counts per second per pixel row), Almelo, Netherlands. A temperature cell (Anton Paar TTK 450 low-temperature chamber and Anton Paar TCU 100 temperature-control unit, Gtaz, AUSTRIA) were used to perform the temperature dependence measurements. The wavelength of the incident X-ray beam was 0.15418 nm (Cu Kα). PAN sample was set in the sample chamber and heated at 10°C/min from 50 to 290°C. A 2θ scan (0–40°) which θ is Bragg angle, and a β scan at 2θ = 17° (β is azimuthal angle, 0–180°) were performed.

Changes in the crystallinity (X_{cry}) and the crystallite size for the PAN fibers throughout the thermal process were calculated with eqs. (3) and (4):[15,16]

$$X_{cry} = \frac{S_{cry}}{S_{amo} + S_{cry}} \times 100\% \quad (3)$$

where S_{cry} and S_{amo} are the integrated intensities of the peaks for the crystalline and amorphous components, respectively:

$$L_{(a)} = \frac{K\lambda}{\beta \cos\theta} \quad (4)$$

where $L_{(a)}$ is the crystallite size along the a axis for the PAN fibers, θ is the Bragg angle of the (100) diffraction, β is the half-width of the (100) diffraction peak at 2θ = 16.9°, K is a constant (0.89), and λ is the wavelength of the Cu Kα radiation.

Orientation degree of the molecular chains

The total orientation degree of the molecular chains in the PAN fibers was determined with an acoustics velocity meter (Chinese Academy of Sciences Instruments). The total orientation degree of the PAN fibers and the orientation degree of the amorphous region were calculated with eqs. (5)–(7).[17–19]

$$f_{sum} = 1 - \frac{{C_u}^2}{{C_x}^2} \quad (5)$$

where f_{sum} is the total chain orientation degree of the PAN fibers, C_u is a constant of acoustics velocity (2.1 km/s) for the PAN fibers with totally

TABLE II
Initial Values for the Four Types of PAN Samples

Sample number	1	2	3	4
Diameter (μm)	14.03	13.30	12.96	11.25
L_0 (mm)	21.64	21.66	21.64	21.63

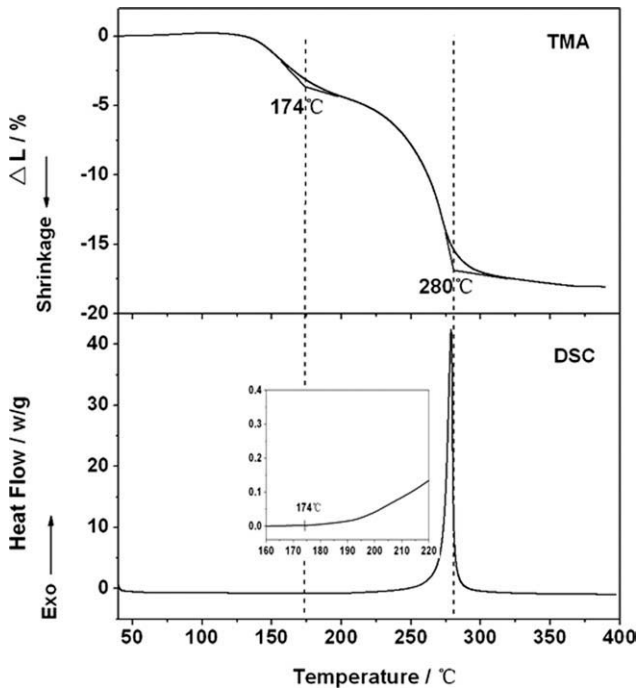

Figure 1 TMA and DSC curves for the PAN fibers at a heating rate of 10°C/min in nitrogen.

disordered molecular chains, and C_x is the measured acoustics velocity for the PAN samples:

$$f_{\text{amo}} = \frac{(E_s - E_u) - X_{\text{cry}} f_{\text{cry}} E_s}{E_s(1 - X_{\text{cry}})} \quad (6)$$

where f_{amo} is the orientation degree of the amorphous region in the PAN fibers, E_u is a constant of acoustics modulus ($11.3C_u^2$), E_s is the measured acoustics modulus for the PAN samples ($11.3C_x^2$), and X_{cry} and f_{cry} are the crystallinity of the PAN fibers and the orientation degree in the crystalline region, respectively:

$$f_{\text{cry}} = \frac{180 - H}{180} \times 100\% \quad (7)$$

where H is the half-width of the peak in the azimuthal scan from X-ray diffraction (XRD) determination.

Fourier transform infrared (FTIR) spectroscopy

FTIR spectroscopy was performed with a Bruker Tensor 27 spectrometer (Ettlingen, Germany) with a temperature cell (Linkam FTIR600). The infrared spectra were obtained with a resolution of 8 cm^{-1} in the wavelength range 4000–400 cm^{-1}. The PAN fibers were fixed in the cell and heated at 10°C/min from 30 to 290°C.

RESULTS AND DISCUSSION

Thermal shrinkage behavior of the PAN fibers

Figure 1 shows the changes in axial shrinkage and the exothermic behavior of the PAN fibers at a heating rate of 10°C/min in nitrogen. With increasing temperature, there were two clear stages in the TMA shrinkage curve. At temperatures below 174°C, the initial step of axial shrinkage was observed. The shrinkage at this stage was approximately 20% of the total shrinkage; meanwhile, there was no visible chemical enthalpy in the DSC curve. This indicated that there was no chemical reaction occurring below 174°C, and the axial shrinkage resulted from the physical motion of the PAN molecular chains.[3]

Above 174°C, a slow exothermic phenomenon was observed by DSC, which reflected the onset of the chemical reaction, especially the cyclization.[20,21] At this time, the secondary shrinkage step appeared in the TMA curve. The results indicate that the molecular chains started crosslinking through cyclization from 174°C; this led to the beginning of chemical shrinkage of the PAN fibers. When the temperature was increased further, the exotherm rose, and the axial shrinkage sharply increased. When the heating temperature was beyond 250°C, the exotherm of cyclization went up rapidly, and a sharp peak at 270°C was observed. The corresponding axial shrinkage of the PAN fibers also increased remarkably. Above 280°C, the exotherm declined, and the growth of axial shrinkage slowly decreased. This indicated that there was a close correlation between the secondary shrinkage and the cyclization degree.

Furthermore, the progressing of cyclization with heating temperature was also supported by the temperature dependence of the IR spectra for the PAN fibers in Figure 2. It was found that below 160°C, the spectra had basically no change; when the heating temperature was above 180°C, the intensity of

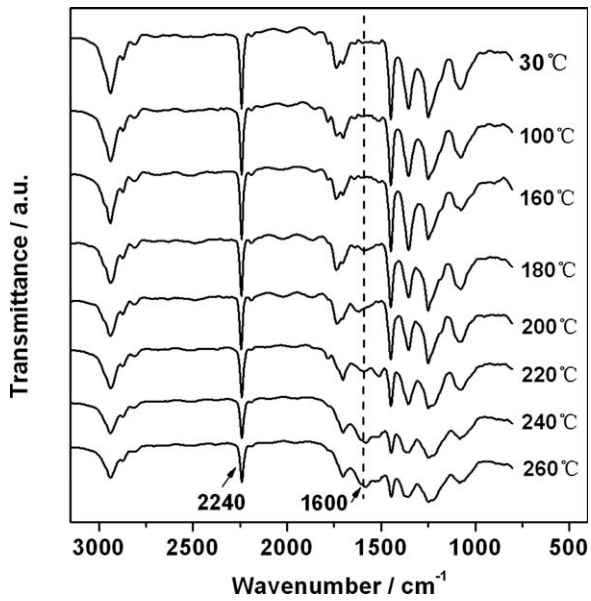

Figure 2 .FTIR spectra for the PAN fibers at a heating rate of 10°C/min.

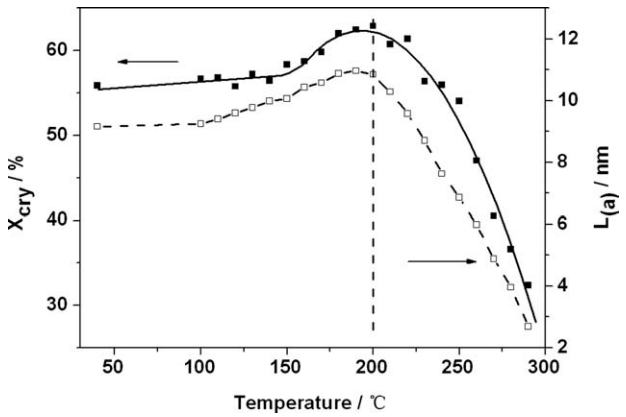

Figure 3 Crystallinity and crystallite size of the PAN fibers at a heating rate of 10°C/min in nitrogen.

the $\nu_{-C\equiv N}$ band (the band at 2240 cm^{-1}) decreased, but that of the $\nu_{-C=N}$ band (the band at 1600 cm^{-1}), which was due to the resultant functional group in the cyclization reaction, increased gradually. This indicated that chemical reactions occurred above 180°C and progressed with higher temperatures.

Figure 3 shows the variation of the crystalline parameters for PAN fibers throughout the secondary shrinkage. The crystallinity increased slowly above 174°C and then decreased rapidly at temperatures above 200°C. The variation in crystallite size was similar to that of the crystallinity. In combination with the TMA results from Figure 1, below 174°C, the PAN fibers shrank by the physical relaxation of molecular chains, whereas the crystallinity and crystallite increased gently in this temperature range. It was considered that when the molecular chains in the amorphous phase shrank, the inner stress of the PAN fibers increased. Under this stress, the orientated molecular chains in the amorphous phase (near the crystalline regions) were orderly rearranged into crystalline regions; this resulted in an increase in the crystallinity and crystallite size.

Above 174°C, the chemical reaction had already started (DSC results in Fig. 1), whereas the crystallinity and crystallite size did not decrease but increased obviously. This meant that the cyclization mainly occurred in the amorphous phase at the beginning of the process, and the crystalline regions had not yet been destroyed by crosslinking. With many molecular chains participating in the cyclization, the inner stress of the PAN fibers grew rapidly, and the crystallinity and crystallite size increased markedly.

When temperature was above 200°C, the molecular chains in the crystalline region took part in the cyclization and began to shrink, the regular crystalline structures were transformed from linear chains to crosslink structures, and the crystallinity and crystallite size decreased correspondingly. With further increasing temperature, the destruction of the crystalline regions accelerated, and both the crystallinity and crystallite size decreased rapidly.

Effect of the aggregation structure on the secondary shrinkage of the amorphous regions

As shown in the TMA curves in Figure 4, PAN fibers with different aggregation structures had different secondary shrinkage behaviors. The changes in aggregation structure throughout the chemical shrinkage for these PAN fibers were monitored by XRD (Fig. 4). With increasing temperature, the crystallinity initially increased and then decreased sharply; this indicated that the process of secondary shrinkage was extended from the amorphous to the crystalline phase. At 200°C, there was a cutoff point in the crystallinity for all of these fibers, and the secondary shrinkage was extended to the crystalline regions from this point onward. It was reasonable to conclude that the shrinkage below 200°C came from the amorphous region.

The differences in the variation of crystallinity for four types of PAN fibers during shrinking process could also be concluded from Figure 4. For fibers with a greater original crystallinity, the crystallinity increased more obviously after molecular chain shrinkage in the amorphous phase (<200°C). It was speculated that for PAN fibers with a greater original crystallinity, there were more orientable molecular chains because of the facile alignment at the

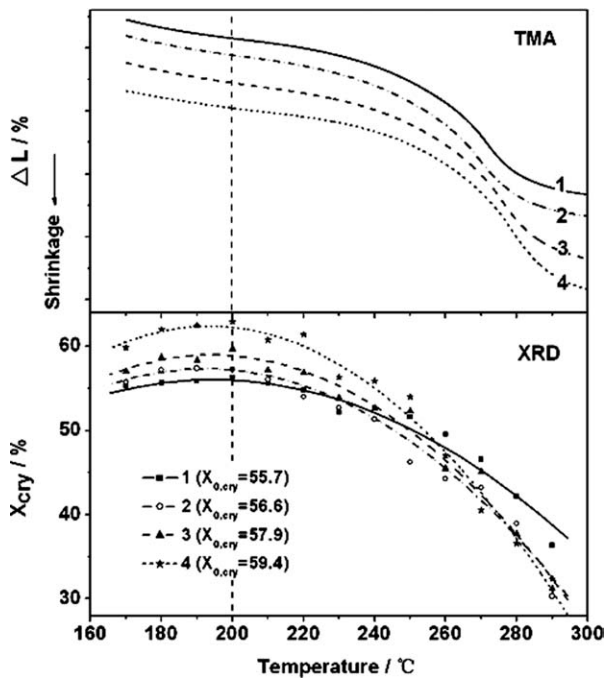

Figure 4 Free shrinkage and crystallinity for four types of the PAN fibers at a heating rate of 10°C/min in nitrogen.

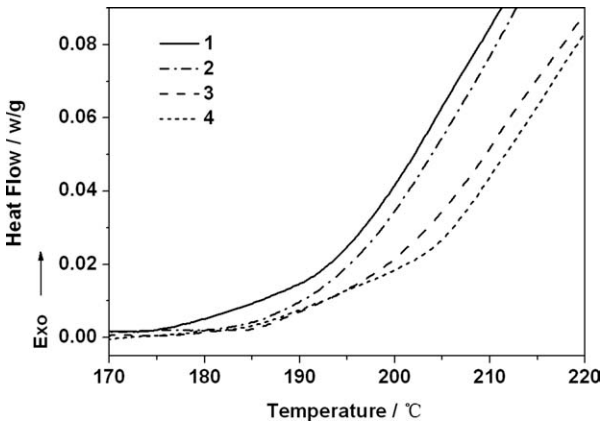

Figure 5 DSC curves for the PAN fibers at a heating rate of 10°C/min in nitrogen.

boundary of the crystalline regions. These molecular chains rearranged into crystalline regions more easily under inner stress, which was brought about by chemical shrinkage in the amorphous phase.

Figure 5 shows the exothermic behavior for PAN fibers with various aggregation structures during cyclization in N_2. The calculated RCD occurring in the amorphous phase (<200°C) for these fibers is listed in Table III. The exothermic enthalpy and RCD were relatively smaller for PAN fibers with a greater crystallinity at a given temperature. On the one hand, when the cyclization occurred mainly in the amorphous phase, the RCD was lower for PAN fibers with a greater crystallinity because of the relatively lower amount of amorphous phase within these fibers; on the other hand, there were more orientated molecular chains near the crystalline regions rearranged to the crystalline phases for PAN fibers that had larger crystallinity (Fig. 4), and the RCD for the cyclization of remnant molecular chains in the amorphous phase was further decreased.

Figure 6 shows both the RCD and chemical shrinkage in the amorphous phase for PAN fibers with different aggregation structures. For a certain PAN fiber, the shrinkage of the amorphous region increased gradually with increasing RCD. In a comparison of PAN fibers with different crystallinities, the shrinkage rates of the amorphous regions were different at same RCD level: $\Delta L_{amo1} < \Delta L_{amo2} < \Delta L_{amo3} < \Delta L_{amo4}$. We considered that by the effects of the aggregation structures, the orientated molecular chains in the amorphous phase shrank more obviously than the disordered molecular chains after

TABLE III
RCD for the Stabilized PAN Fibers in the Amorphous Phase (<200°C)

Sample number	1	2	3	4
RCD (%)	0.38	0.28	0.19	0.17

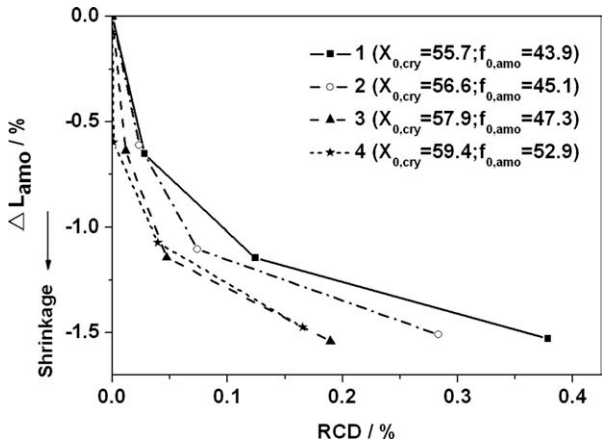

Figure 6 Chemical shrinkage variation with RCD for the four types of PAN fibers (ΔL_{amo} = chemical shrinkage of the amorphous region).

crosslinking. Therefore, sample 4, which had a higher orientation degree of molecular chains in the amorphous phase, shrank more than the other samples when the RCD values were the same. Although the crystallinity influenced RCD in the amorphous phase, it was not the only factor affecting the secondary shrinkage rate in the amorphous phase. The secondary shrinkage was also associated with the orientated molecular chains in the amorphous phase.

Effect of the aggregation structure on the secondary shrinkage of the crystalline phase

Figure 7 shows the variations in chemical shrinkage extending into the crystalline phase for PAN fibers with different aggregation structures. Compared to that in the amorphous phase, the shrinkage in the crystalline region (>200°C) was much more remarkable and was larger for PAN fibers with greater crystallinities. With the aggregation structure

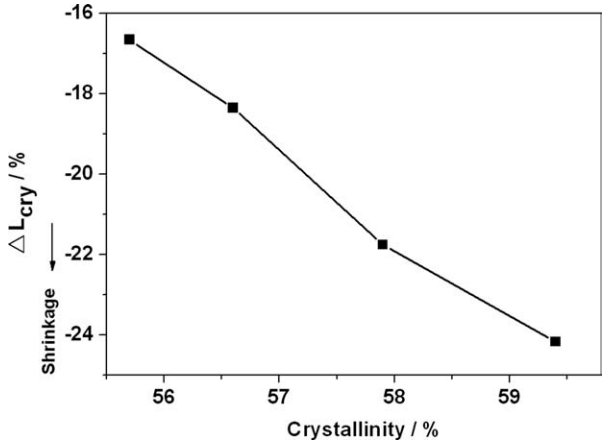

Figure 7 Chemical shrinkage of crystalline region for the PAN fibers with different crystallinities (ΔL_{cry} = chemical shrinkage of the crystalline region).

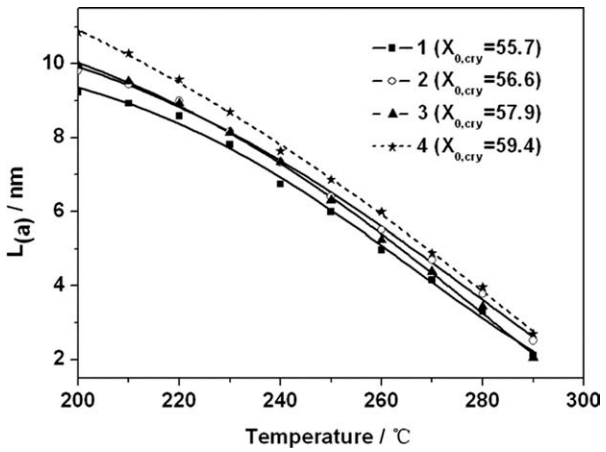

Figure 8 Crystallite size for four types of PAN fibers at a heating rate of 10°C/min in nitrogen (200–290°C).

character taken into account, there were many random molecular chains in the amorphous phase, most of which participated in the cyclization and shrank less by crosslinking. Conversely, there were many more orientated molecular chains in the crystalline phase. When these chains participated in cyclization, the original rigid crystalline structure was gradually destroyed, the confinement effect of these crystalline structures on the mobility of the molecular chains was decreased, and the shrinkage rate in the crystalline region increased rapidly.

The variation in crystallite size for PAN fibers with different aggregation structures during chemical reactions occurring in the crystalline regions is shown in Figure 8. The crystallite size decreased obviously after the regular crystalline structures were destroyed by crosslinking. This was similar to the variation in crystallinity with increasing temperature (Fig. 4). When the heating temperature was over 290°C, the crystallite sizes for all of these fibers decreased to almost 2 nm. It was clearly found that

TABLE IV
Total RCD for the Four Types of Stabilized PAN Fibers (174–300°C)

Sample number	1	2	3	4
Peak temperature (°C)	273.3	275.1	276.7	279.2
RCD (%)	97.03	97.14	97.21	97.29

the crystallite size decreased more remarkably for PAN fibers with larger original values.

Figure 9 shows the cyclization exothermic character of the crystalline region for PAN fibers with different aggregation structures. At temperatures over 200°C, the remaining linear molecular chains in the amorphous phase were cyclized and decreased in amount, whereas RCD in the crystalline region increased gradually. As shown in Figure 9, the total heat increased more sharply in the later stage of cyclization for PAN fibers with greater crystallinity. It was considered that by the effect of the aggregation structures on the mobility of the molecular chains, these chains, which arranged more regularly in the complete crystalline regions, began cyclizing under higher temperatures, and their cyclization was relatively intense.

The calculated RCDs for the four types of PAN fibers during heat treatment from 200 to 300°C are listed in Table IV. RCD for PAN fibers with greater crystallinity was larger. Because RCD for cyclization occurring in the amorphous phase was lower for PAN fibers with less amorphous phase content (Table III), it was speculated that RCD in the crystalline phase would be larger for those with a relatively greater crystalline phase content.

Figure 10 shows the RCD and chemical shrinkage in the crystalline phases for PAN fibers with different aggregation structures. The chemical shrinkage for all of these fibers increased gradually at the

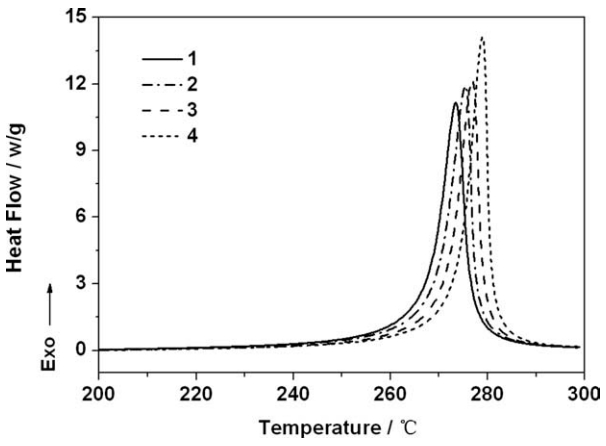

Figure 9 DSC curves for the PAN fibers with different aggregation structures at a heating rate of 10°C/min in nitrogen (200–300°C).

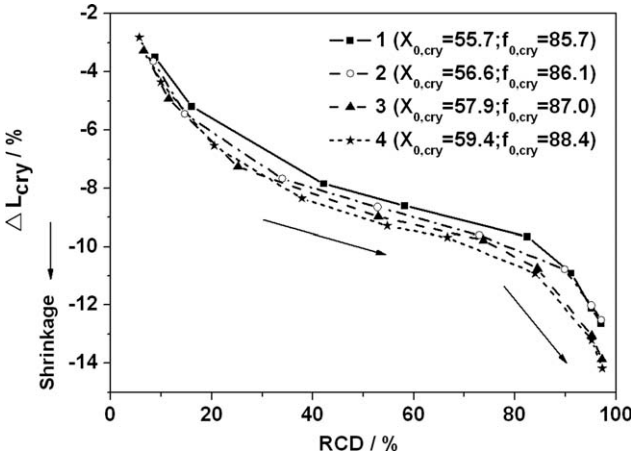

Figure 10 Chemical shrinkage variation with RCD for the PAN fibers with different aggregation structures (ΔL_{cry} = chemical shrinkage of the crystalline region).

beginning and then grew quickly with increasing RCD. It was indicated that in the later stage of cyclization, a large number of orientated molecular chains in the crystalline regions participated in cyclization, the original crystalline regions were destroyed, and the shrinkage increased rapidly as a result. Overall, PAN fibers with a higher crystallinity had a larger RCD in the crystalline region, the chemical shrinkage increased more obviously through molecular chain crosslinking, and the total shrinkage was much larger.

In a comparison of different PAN fibers, the secondary shrinkages of the crystalline phases were different when RCDs of these fibers reached to the same level: $\Delta L_{amo1} < \Delta L_{amo2} < \Delta L_{amo3} < \Delta L_{amo4}$. It was speculated that the orientation degree of the crystalline region influenced the shrinkage in the crystalline regions. PAN fibers with a larger orientation degree of crystalline region (sample 4) had a relatively larger shrinkage under the same cyclization degree.

CONCLUSIONS

The secondary shrinkage behavior of PAN fibers was not only associated with the degree of cyclization but also depended on the mobility of molecular chains in the aggregation structures during heat crosslinking. With increasing temperature, the molecular chains in the amorphous phase first participated in cyclization and started to generate the secondary shrinkage. As most molecular chains in the amorphous phase had random alignment, the changes in length were relatively small. At temperatures above 200°C, the molecular chains in the crystalline regions started to undergo cyclization, and the shrinkage at this stage was increased because of the larger content of orientated molecular chains, which shrank by crosslinking.

For certain PAN fibers, the overall shrinkage increased gradually at first and then more rapidly with increasing cyclization degree. As the molecular chains, which arranged more regularly in the complete crystalline regions, needed higher temperatures to start cyclizing, the chemical shrinkage of these chains was observed later and was relative larger, so the shrinkage in the crystalline region increased quickly in the later stage of cyclization.

For PAN fibers with different aggregation structures, the shrinkage in both the amorphous and crystalline regions increased with more orientated molecular chains in these regions under the same cyclization degree. The crystallinity affected the cyclization degree but did not directly affect the overall shrinkage. As the random molecular chains shrank smaller after cyclization, the total shrinkage was mainly affected by the content of orientated molecular chains that participated in the cyclization. PAN fibers that had a larger crystallinity and crystalline orientation degree had a larger overall shrinkage.

References

1. Warner, S. B.; Peebles, L. H., Jr.; Uhlmann, D. R. J Mater Sci 1979, 14, 565.
2. Jain, M. K.; Bala, M.; Desai, P.; Abhiraman, A. S. J Mater Sci 1987, 22, 301.
3. Fitzer, E.; Frohs, W.; Heine, M. Carbon 1986, 24, 387.
4. Wu, G. P.; Lu, C. X.; Wu, X. P. J Appl Polym Sci 2004, 94, 1705.
5. Bahl, O. P.; Manocha, L. M. Angew Macromol Chen 1975, 48, 145.
6. Fitzer, E.; Muller, D. J. Macromol Chem 1971, 144, 117.
7. Watt, W.; Johnson, W. Appl Polym Sym 1969, 13, 215.
8. Layden, G. K. J Appl Polym Sci 1971, 15, 1709.
9. Bahl, O. P.; Mature, R. B. Fiber Sci Technol 1979, 12, 31.
10. Wang, P. H. J Appl Polym Sci 1997, 67, 1185.
11. Wu, G. P.; Lu, C. X. J Appl Polym Sci 2005, 96, 1029.
12. Yu, M. J.; Wang, C. G. J Appl Polym Sci 2006, 102, 5500.
13. Hou, Y. P.; Sun, T. Q.; Wang, H. J.; Wu, D. J Appl Polym Sci 2009, 114, 3668.
14. Her, F. Carbon Fibers and Graphite Fiber; Chemical Industry Press: Beijing, 2010.
15. Yu, M. J.; Wang, C. G.; Bai, Y. J.; Wang, Y. X. Polym Bull 2006, 57, 525.
16. Jing, M.; Wang, C. G. Polym Bull 2007, 58, 541.
17. Zhao, H. S.; Jiang, J. D.; Wu, D. C. Polymer Physics; Textile Industry Press: Beijing, 1982.
18. Hu, X. C.; Shao, H. L.; Liang, Y. J. Chin Acad J Elec Pub Hou 1991, 3, 2.
19. Zhou, G. N. Polymer X-ray Diffraction; Chinese Science and Technology University Press: Hefei, 1989.
20. Klimenko, I. B.; Platonova, N. V.; Tarakanova, B. M. Maiburov Fibre Chem 1993, 25, 453.
21. Kakida, H.; Tashiro, K. Polym J 1997, 29, 557.